



**HAL**  
open science

# Magnetic and electronic properties of bulk and clusters of FePtL1\_0

Cyrille Barreateau, Daniel Spanjaard

► **To cite this version:**

Cyrille Barreateau, Daniel Spanjaard. Magnetic and electronic properties of bulk and clusters of FePtL1\_0. *Journal of Physics: Condensed Matter*, 2012, 24, pp.406004. 10.1088/0953-8984/24/40/406004 . hal-00864636

**HAL Id: hal-00864636**

**<https://hal.science/hal-00864636>**

Submitted on 23 Sep 2013

**HAL** is a multi-disciplinary open access archive for the deposit and dissemination of scientific research documents, whether they are published or not. The documents may come from teaching and research institutions in France or abroad, or from public or private research centers.

L'archive ouverte pluridisciplinaire **HAL**, est destinée au dépôt et à la diffusion de documents scientifiques de niveau recherche, publiés ou non, émanant des établissements d'enseignement et de recherche français ou étrangers, des laboratoires publics ou privés.

# Magnetic and electronic properties of bulk and clusters of FePtL<sub>10</sub>.

**Cyrille Barreateau**

CEA, IRAMIS, SPCSI, F-91191 Gif sur Yvette, France

**Daniel Spanjaard**

Laboratoire de Physique des Solides, Université Paris Sud, Batiment 510, F-91405 Orsay, France

E-mail: [cyrille.barreateau@cea.fr](mailto:cyrille.barreateau@cea.fr)

**Abstract.** An efficient tight-binding model including magnetism and spin-orbit interactions is extended to metallic alloys. The tight-binding parameters are determined from a fit to bulk *ab-initio* calculations of each metal and rules are given to get the heteroatomic parameters. Spin and orbital magnetic moment as well as magneto-crystalline anisotropy are derived. We apply this method to bulk FePt L<sub>10</sub> and the results are compared with success to *ab-initio* ones when existing. Finally this model is applied to a set of FePt L<sub>10</sub> clusters and physical trends are derived.

PACS numbers: 71.15.-m, 71.20.Be, 75.30.Gw, 75.75.Lf

## 1. Introduction

Metallic nanoparticles are now the subject of extensive investigations in view of both their technical applications and theoretical interest. It is now well known that such clusters have physical and chemical properties which differ from bulk matter or individual atoms. In this respect nanoalloys are fascinating since their properties may be tuned by varying their composition and size. In particular an increasing number of works have been devoted to equiatomic FePt nanoparticles (see for example Ref.[1] and references therein) since the bulk phase is ferromagnetic with a large magneto-crystalline anisotropy and it is hoped that this property will survive in small clusters so that superparamagnetism can be avoided. Then FePt nanoparticles could be used for high density memories [2] since, from a practical point of view, there are many chemical ways of synthesizing these particles with a small dispersion of size [3, 4]. Note also that by adding functional groups at the surface, FePt has potential application for radio guided targeting and imaging of cancer [5].

In this paper we present a systematic theoretical investigations of the magnetic properties of FePt L1<sub>0</sub> clusters as a function of their size and geometry. The paper is organized as follows. In the next section we present the models used. Section 3 concerns the determination of parameters. In section 4 the results obtained for the bulk are described. Section 5 is devoted to the study of clusters. Finally the summary and conclusion are given in section 6

## 2. Model

We have used an hamiltonian based on a tight-binding model (TB) which we will now briefly describe. More details can be found in [6]. Let us start with a metal made of a single chemical element. The hamiltonian is divided in four contributions:

$$H = H_{TB} + H_{SO} + H_{Stoner} + H_{NC} \quad (1)$$

The first term  $H_{TB}$  is the non-orthogonal tight-binding hamiltonian. It contains three kinds of term the first one is the atomic level (i.e. the intra-atomic term)  $\langle i, \lambda | H | i, \lambda \rangle$ , where  $|i, \lambda\rangle$  is the orbital  $\lambda$  on site  $i$ ,  $\lambda$  being  $s, p$  and  $d$  valence orbitals. This term is parametrized as a function of the atomic environment in the work of Mehl and Papaconstantopoulos [7] by the following expression:

$$\varepsilon_{i,\lambda} = a_\lambda + b_\lambda \rho_i^{2/3} + c_\lambda \rho_i^{4/3} + d_\lambda \rho_i^2 \quad (2)$$

$a_\lambda, b_\lambda, c_\lambda, d_\lambda$  being parameters to be determined. The expression of  $\rho_i$  is related to the atomic density around the atom  $i$  and is given by [7]:

$$\rho_i = \sum_{j \neq i} \exp[-\Lambda^2 R_{i,j}] F_c(R_{ij}) \quad (3)$$

where  $\Lambda$  is a parameter and  $F_c(R)$  is a cut-off function. In order to increase the accuracy of our calculations we have found useful to add an extra term  $e_\lambda \rho_i^{1/3}$  in the expression of  $\varepsilon_{i,\lambda}$ ,  $e_\lambda$  being a new parameter. The remaining terms are the

hopping integrals  $\beta_{i\lambda,j\mu} = \langle i, \lambda | H | j, \mu \rangle$  and the overlap integrals  $S_{i\lambda,j\mu} = \langle i, \lambda | j, \mu \rangle$ . Each of these integrals are given as a function of 10 Slater-Koster [8] parameters:  $ss\sigma, sp\sigma, sd\sigma, pp\sigma, pp\pi, pd\sigma, pd\pi, dd\sigma, dd\pi, dd\delta$ . These parameters decrease exponentially with distance and are written themselves as analytic functions depending on several parameters in Ref.[7].

The term  $H_{SO}$  in the expression of the hamiltonian corresponds to the spin-orbit interactions. It can be written:

$$H_{SO} = \sum_i \xi \vec{L}_i \cdot \vec{S}_i \quad (4)$$

with:

$$\xi = \int_0^\infty R_i^2(r) r^2 dr \quad (5)$$

where  $R_i$  is the radial part of the considered atomic orbital at site  $i$ ,  $\vec{L}_i$  is the orbital momentum operator with respect to the center  $i$  and  $\vec{S}_i$  is the spin operator. In the following we will only consider the  $d$  orbitals in  $H_{SO}$  and ignore the  $p$  orbitals since their influence on the magnetic peoperties is negligible.

The hamiltonian described so far is non magnetic. A simple way of introducing magnetism is given by the Stoner hamiltonian  $H_{Stoner}$  in Eq 6

$$H_{Stoner} = -1/2 \sum_{i\lambda} I_{i\lambda} \vec{m}_{i\lambda} \cdot \vec{\sigma} \quad (6)$$

where  $I_{i\lambda}$  is the Stoner factor for the orbital  $\lambda$  on site  $i$ ,  $m_{i\lambda}$  is the corresponding magnetic moment and  $\vec{\sigma} = (\sigma_x, \sigma_y, \sigma_z)$  are the Pauli matrices. Note that in this work we do not assume the collinearity of all spin moments.

The last term in the expression of the hamiltonian  $H$  can be written:

$$H_{NC}^{i\lambda,j\mu} = \frac{1}{2} (U_i(n_i - n_i^0) + U_j(n_j - n_j^0)) S_{i\lambda,j\mu} \quad (7)$$

in which  $n_i$  is the Mulliken charge of atom  $i$  and  $n_i^0$  the atomic charge.  $U_i$  is the so-called Coulomb energy of atom  $i$  which amplitude controls the size of the charge transfer. The role of these terms is the following : the clusters being an inhomogeneous atomic system the various values of the atomic levels may lead to an important charge transfer between atoms which, in a metal, is unphysical. Thus the presence of  $H_{NC}$  in the hamiltonian limits such charge transfers.

If we consider now a metallic alloy made of two chemical elements, the values of heteroatomic hopping and overlap integrals are obtained as the arithmetic average of the corresponding homonuclear quantities. Concerning the intra-atomic terms we have been able to perform separately a fit for both chemical elements with the same value of  $\Lambda$ . The intra-atomic term of a given atom in the system will then only depend on the nature of the considered atom by the coefficients  $a_\lambda, b_\lambda, c_\lambda, d_\lambda$  and  $e_\lambda$ .

We have also found that the electronic and magnetic properties of the bulk alloy are reproduced more closely if we fix the number of  $d$  electrons of the two elements by adding to  $H$  the following hamiltonian (that applies to  $d$  orbitals only):

$$H_{NCd}^{i\lambda,j\mu} = \frac{1}{2} (U_{d,i}(n_{id} - n_{id}^0) + U_{d,j}(n_{jd} - n_{jd}^0)) S_{i\lambda,j\mu} \quad (8)$$

$n_{id}$  and  $n_{id}^0$  being respectively the  $d$  charge of atom at site  $i$  and this charge in the bulk. Actually  $n_{id}^0$  is taken as a parameter to be adjusted but is close to the one obtained from ab-initio calculations.

The total energy of the system is written similarly to Mehl and Papaconstantopoulos[7] as the sum of the occupied one electron eigenvalues  $\varepsilon_\alpha$ . The total energy should also be modified by the so-called double counting terms arising from the electron-electron interactions introduced by the Stoner and charge neutrality terms. The total energy then reads:

$$E_{\text{tot}} = \sum_{\alpha} f_{\alpha} \varepsilon_{\alpha} - \sum_i \frac{U_i}{2} (n_i^2 - (n_i^0)^2) - \sum_i \frac{U_{d,i}}{2} (n_{d,i}^2 - (n_{d,i}^0)^2) + \sum_{i\lambda} \frac{I_{i\lambda}}{4} m_{i\lambda}^2 \quad (9)$$

$f_{\alpha}$  being the occupation of state  $\alpha$ . Note that the expression of  $H$  depends on charges which are given by its eigenfunctions thus, the diagonalization of this matrix should be done self-consistently. Let us finally insist on the fact that within this approach we are not fitting any DFT data from the bi-metallic system to determine new TB parameters. The only slight adjustment that is made is the one to determine the  $n_{id}^0$  parameters.

### 3. Determination of parameters

As in the work of Mehl and Papaconstantopoulos [9] all the parameters involved in  $H_{\text{TB}}$  for the pure chemical element are determined by a least mean square fit of the results of non magnetic ab-initio band structure calculations for several lattice parameters, in the absence of spin-orbit interactions. Generalized gradient approximation (GGA) has been used for Fe since it is well known that its use is necessary to reproduce the right bulk phase of iron while for Pt we have preferred the Local density approximation (LDA) which gives a lattice parameter in better agreement with experiment[10]. This fit, shown on Fig.1 for the equilibrium lattice parameter of Pt, is excellent. The same kind of agreement is obtained for Fe.

The spin-orbit constants  $\xi_{Fe}$  and  $\xi_{Pt}$  were determined by comparison with the band structure calculated from the same ab-initio code including now the spin-orbit coupling. This fit is presented in Fig.2. The agreement between both calculations is very satisfying. One finds  $\xi_{Fe} = 0.06eV$  and  $\xi_{Pt} = 0.57eV$ .

We must now determine the Stoner parameters. In transition metal the spin magnetic moment has essentially a  $d$  character. Accordingly we have taken  $I_s = I_p = I_d/10$ . The value of  $I_d$  is again obtained by comparison with ab-initio calculations. The magnetic moment is computed as a function of the lattice parameter for several values of  $I_d$ . The corresponding curves are shown in Fig.3 for Fe in a BCC structure. A good estimate of the Fe Stoner parameter  $I_d(Fe)$  range between  $0.88eV$  and  $0.95eV$ . In the rest of the paper both values have been considered. The same kind of agreement for Pt in a FCC structure including or not the spin-orbit interactions is obtained for a Stoner parameter  $I_d(Pt) = 0.6eV$ . In this last case the value of the Stoner parameter has

been chosen so that the lattice parameter for which the magnetism appears coincide (See Fig. 3) in both computations in the absence of spin-orbit interactions. Note that these values of the Stoner parameter are quite close to those which can be deduced from the LSDA+U calculations of Schick and Mryasov [11] on FePt:  $I_d(Fe) = 0.98eV$  and  $I_d(Pt) = 0.54eV$ . In addition it can be seen from Fig. 3 that the spin-orbit coupling of Platinum has a strong influence on the onset of the spin moment which appears for larger values of the lattice parameter.

#### 4. Results for bulk FePt L1<sub>0</sub>

In order to check the validity of our model, we have computed several physical quantities and compared them to the results provided by *ab-initio* methods.

Bulk FePt orders in the L1<sub>0</sub> structure in which the (001) planes of the fcc lattice are alternatively occupied by Fe and Pt atoms. This ordering induces a contraction along the  $\langle 001 \rangle$  fcc axis (denoted as the  $c$  axis) changing the ratio  $c/a$  ( $a$  being the nearest neighbor distance in the (001) plane) from the fcc value of  $\sqrt{2}$ . Indeed it is found experimentally that  $a = 2.73\text{\AA}$  and  $c = 3.72\text{\AA}$  so that  $c/a = 1.36$ .

Let us now discuss the magnetic properties of FePt. Experiments have found that bulk FePt is ferromagnetic (FM). Assuming this magnetic order, we have computed the magnetic moments of Fe and Pt of this alloy taking  $U = U_d = 20eV$  and adjusting  $n_{Fe,d}^0$  and  $n_{Pt,d}^0$  to reproduce the moments given by our *ab-initio* calculations, i.e.  $\mu(Fe) = 2.8\mu_B$  and  $\mu(Pt) = 0.37\mu_B$ . One finds:  $n_{Fe,d}^0 = 6.6$  and  $n_{Pt,d}^0 = 8.3$ . Note that these values of  $n_{i,d}^0$  are quite comparable to those given by Antoniak *et al.*:  $n_{Pt,d}^0 = 8.3$  and  $n_{Fe,d}^0 = 6.6$  [12]. It is interesting to shed some light on the influence of  $U_d$  on these results. It can be seen on Fig.4 that when  $U_d$  increases the spin moment of Fe increases rapidly and then saturates at  $\mu(Fe) = 2.86\mu_B$  for  $U_d = 20eV$  while the moment  $\mu(Pt)$  of Pt decreases and reach a plateau at  $0.39\mu_B$  for the same value of  $U_d$ . This is due to an electronic transfer from Fe to Pt when  $U_d$  increases. Keeping  $U_d = 20eV$  we have computed the  $d$  density of states of the up and down spin bands and compared the results to our DFT calculations. As can be seen on Fig.5 the agreement between both results is very satisfying.

However several calculations [13, 14] did show that there is a competition between ferromagnetism and antiferromagnetism (AFM) of the alternating Fe planes. Although the exchange coupling within the Fe layers is strong and ferromagnetic, it is weakly antiferromagnetic between Fe layers [15]. However the induced moments on the Pt sites give rise to an effective interaction which favors the FM order. As a result the difference in energy between the two orders is quite small. In order to verify this point we have done the following calculations. We have computed the energy per atom as a function of the lattice parameter in a FM and AFM configuration for the two values of the Fe Stoner parameter, i.e.,  $I_d(Fe) = 0.95eV$  and  $I_d(Fe) = 0.88eV$ , using our tight-binding code and compared the results with those of Quantum-espresso *ab-initio* package[16] in LDA and GGA. This comparison is shown in Fig.6. As can be seen on this figure, it is

found that LDA and TB results are very close for  $I_d(Fe) = 0.88$ . However both find an AFM order for the experimental lattice parameter, the energy difference between (FM) and (AFM) orders being of a few meV and decreases when  $I_d(Fe)$  increases. On the contrary GGA results are somewhat different and show that the FM order is stabilized but at a lattice parameter which is slightly larger than the experimental one. If the  $d$  charge neutrality is not taken into account, i.e. if  $U_d = 0$ , the energy of the AFM order is far above the FM one for  $I_d(Fe) = 0.88eV$  as well as for  $I_d(Fe) = 0.95eV$ . In addition we have computed, using the TB code, the energy per atom as a function of  $c/a$  at fixed  $a = 2.7\text{\AA}$  value for the same two values of the Stoner parameter (see Figs 7). For both Stoner parameters the minimum of energy is obtained for the AFM order at  $c/a \approx 1.35$  however the crossing of FM and AF curves occurs at slightly different values of  $c/a$ . For  $I_d(Fe) = 0.95eV$  the minimum of energy of the FM curve is obtained at  $c/a = 1.37$  and for this fixed value of  $c/a$  the FM order is slightly favored. As a general trend one can note that increasing  $c/a$  favors ferromagnetism.

An other very interesting quantity is the magneto-crystalline anisotropy energy (MAE) i.e., the difference in energy per formula unit between magnetic moments pointing parallel and perpendicular to the  $c$  axis. This quantity being much smaller than each member of the difference its calculation is very delicate and constitute therefore a very good test of our model. We have computed this MAE as a function of the ratio  $c/a$  for a fixed unit cell volume in the FM configuration and  $I_d(Fe) = 0.88eV$ . The results are shown in Fig.8 and closely resemble those carried out by Lyubina *et al.* [17] (see Fig 1 of this reference) using an LSDA *ab-initio* code including spin-orbit interactions. The easy magnetization axis is along  $Oz$  as in experiment but the MAE is too large, nearly by a factor of two at the experimental value of  $c/a$ . Finally we have found that a variation of  $I_d(Fe)$  of about 20% leaves the MAE nearly unchanged. In addition a decrease of  $\xi_{Pt}$  from 0.57eV to 0.45eV lowers the MAE from 3.7meV to 2.5meV.

## 5. Magnetic properties of clusters $L1_0$

All considered clusters are a fragment of an fcc lattice and the (001) central plane is assumed to be made of Fe atoms. The clusters we have considered are of two types as shown in Fig.9. The first type is a closed shell cuboctahedron cluster ( $N=55, 147$ ), which, starting from a central atom, is built by adding its twelve nearest neighbors which gives the first shell. Then, the second shell is obtained by adding the missing nearest neighbors of the atoms of the first shell and the process is iterated until the desired number of shell is attained. These clusters are homothetic and present eight (111) like triangular and six (001) like square facets. The second type of clusters are spherical and are built from a central atom by adding its successive shell of neighbors until a given radius ( $N=19, 43, 55, 79, 87, 135, 141$ ). Note that the  $N = 55$  cuboctahedron cluster belongs also to this family which is not the case of the  $N = 147$  cuboctahedron. This type of construction leads to the formation of cluster structures with sizes, shapes and surface termination different from the closed shell ones. We will see in the following

that this will influence the FM or AFM magnetic order.

We have performed a series of TB calculations for all these clusters at three different  $c/a$  values and the two values of  $I_d(Fe)$ . Atomic relaxations are ignored since our main goal is to obtain general trends and moreover, apart from very small clusters, relaxation effects should have relatively modest effects on the magnetic properties of compact aggregates built from (slightly distorted) fragments of fcc lattice. In each case the initial magnetic order was chosen to be FM or AFM in a collinear state and along the  $Oz$  or  $Ox$  direction. During the self consistent process the directions of the spins are modified but remain not far from collinearity. We have faced convergence problems in some cases concerning metastable states, in particular for the cluster  $N = 141$  in the AF configuration and the cluster  $N = 147$  in the FM configuration. The corresponding energies shown in Fig. 10 and Fig. 13 are questionable.

Let us discuss the magnetic properties of these clusters. It is seen in Fig.10 that, whatever the size of the cluster, increasing the Fe Stoner parameter  $I_d(Fe)$  or the ratio  $c/a$  favors the FM order. For all investigated clusters a FM ground state is found except for the clusters of size  $N=135$  and  $N=147$  if  $I_d(Fe) = 0.88$  and of size  $N = 147$  only if  $I_d(Fe) = 0.95$ .

Let us focus on the case of the  $N = 135$  cluster (see Fig. 11) in the FM and AFM configuration. The spin and orbital magnetic moments decomposed according to the distance  $d$  from the cluster center are shown in Fig.12. Note that atoms at the same distance  $d$  are not necessarily equivalent and therefore do not bear the same magnetic moment as can be seen on Fig 12: it is the case of the couple of atoms ( $Pt_3, Pt_4$ ) and ( $Pt_5, Pt_6$ ) as well as ( $Fe_2, Fe_3$ ) and ( $Fe_5, Fe_6$ ). In the FM configuration the central and outermost Fe atoms have a slightly larger spin moments than the other atoms and not far from the bulk one. This is in very good agreement with DFT calculations performed by Ebert *et al* [18] (see Fig. 1 of their paper). The same behavior is observed in the AFM ordering. It is also seen that the spin moment of the Pt atoms increases with  $d$  in the FM case and in the AFM case the spin moments of the Pt atoms between AFM Fe layers nearly vanish. However in the  $N = 135$  cluster as in the  $N = 141$  cluster the Pt atoms which cover completely the two (001) surfaces have a non negligible spin moment of the same sign as the neighboring Fe layer in accordance with the positive exchange coupling between Pt and Fe atoms found in first-principles calculations [15]. This effect certainly favors the AFM configuration of this cluster as well as for the  $N = 147$  cluster. On the other hand the presence of Fe atoms on the first or last (001) layer of Pt atoms leads to a FM order as in the  $N = 19, 43, 55, 141$  clusters.

Let us consider now the orbital moment of the  $N = 135$  cluster in both the FM and AFM configuration. It can be seen in Fig.12 that when  $d$  increases the orbital moment of the Fe atoms remains small, as expected from the small value of the spin-orbit constant, and most of the time negative. On the contrary the orbital moment of Pt atoms increases dramatically with  $d$  in the FM as well as in the AFM order especially for the surface atoms. This is due to the high value of the spin-orbit constant and to the decrease of the site symmetry when  $d$  increases.



The MAE of the considered clusters as a function of their number of atoms are given in Fig.13 for  $I_d(Fe) = 0.88\text{eV}$  as well as  $I_d(Fe) = 0.95\text{eV}$  and for  $c/a = 1.35, 1.37$  and  $\sqrt{2}$ . When  $I_d(Fe) = 0.95\text{eV}$  the MAE does not vary noticeably with the ratio  $c/a$  and the easy axis of magnetization is along  $Oz$  for all the clusters in the FM order. The same conclusion apply for  $I_d(Fe) = 0.88\text{eV}$  save for the N=135 cluster. In the AFM order the MAE exhibit oscillations as a function of the size of the cluster however the easy axis of magnetization is mainly along  $Ox$ . Finally in Fig.14 the MAE, per formula unit, of the clusters as a function of their size is compared with the bulk MAE. In this calculation the volume of the cluster is approximated by giving to Fe and Pt their respective Wigner-Seitz sphere. It is seen that this last quantity is larger in absolute value than in the small clusters, i.e. for  $N \approx 135$ .

## 6. Conclusions

We have found a non-orthogonal *spd* tight-binding parametrization of Fe and Pt, including spin-orbit interactions, which has been deduced from a fit to non magnetic *ab-initio* calculations as in Ref.[7]. The quality of the fit is excellent. Magnetic effects has been obtained by adding a Stoner term to the hamiltonian. We have shown how this parametrization can be generalized to alloys. In this last case an additional potential is introduced to prevent unphysical large transfer between chemically or geometrically different atoms.

This method has been first applied to FePtL<sub>10</sub> in the bulk phase and the comparison with results from *ab-initio* calculations, when existing, is very satisfying. The case of clusters have then be studied and the following physical trends have been found: (i) there is a competition between FM and AFM order as in the bulk

(ii) increasing the Stoner parameter or the ratio  $c/a$  favors the FM order

(iii) a terminal (001) Pt plane which covers completely the Fe plane favors the AFM order while the presence of Fe atoms on this Pt plane leads to a FM order

(iv) In the FM order the easy axis of magnetization is always along  $Oz$

In conclusion we have set-up an efficient and precise tight-binding approach for alloys which, being much less computer demanding than *ab-initio* calculations, is able to treat complex alloy systems with a very large number of atoms which are presently out of reach of *ab-initio* calculations.

## Acknowledgments

- [1] C. Antoniak and M. Farle 2007 Mod. Phys. Letters B **21** 1111
- [2] C-K. Yin, M. Murugesan, J-C. Bea, M. Oogane, T. Fukushima, T. Tanaka, S. Kono, S. Samukawa and M. Koyanagi 2007 Jap. J. App. Phys. **46** 2167
- [3] Shouheng Sun, C.B. Murray, D. Weller, L. Folks and A. Moser 2000 Science **287** 1989
- [4] V. Tzitzios, G. Basina, L. Colak and D. Niarchos 2011 J. Appl. Phys. **109** 07A718
- [5] G. Hariri, M.S. Wellons, W.H. Morris III, C.M. Lukehart and D.E. Hallahan 2011 Annals of Biomedical engineering **39** 946
- [6] G. Autès, C. Barretau, D. Spanjaard and M.C. Desjonquères 2006 J. Phys.: Cond. Mat. **18** 6785

- [7] M.J. Mehl and D.A. Papaconstantopoulos 1996 Phys. Rev.B **54** 4519
- [8] J. Slater and G. Koster 1954 Phys. Rev. **94** 1498
- [9] M.J. Mehl and D.A. Papaconstantopoulos URL <http://cst-www.nrl.navy.mil/>
- [10] S. Baud *et al* 2004 Phys. Rev. B **70** 235423 .
- [11] A. Shick and O.N. Mryasov 2003 Phys. Rev.B **67** 172407
- [12] C. Antoniak, J. Lindner, M. Spasova, D. Sudfeld, M. Acet, M. Farle, K. Fauth, U. Wiedwald, H.-G. Boyen, P. Ziemann, F. Wilhelm, A. Rogalev, and Shouheng Sun 2006 Phys. Rev. Lett. **97** 117201
- [13] G. Brown, B. Kraczek, A. Janotti, T.C. Schulthess, G.M. Stocks and D.D. Johnson 2003 Phys. Rev.B **68** 052405
- [14] Zhihong Lu, R.V. Chepulskii and W.H. Butler 2010 Phys. Rev.B **81** 094437
- [15] O.N. Mryasov 2004 J. Mag. Mag. Mat. **272-276** 800-801
- [16] Paolo Giannozzi *et al.* 2009 J. Phys. : Cond. Matt. **21** 39
- [17] J. Lyubina, I. Opahle, K.M. Müller, O. Gutfleisch, M. Richter, M. Wolf and L. Schultz 2005 J. Phys.: Cond. Matt. **17** 4157
- [18] H. Ebert, S. Bornemann, J. Minr, P.H. Dederichs, R. Zeller, I. Cabriab, 2006 Comput. Mat. Sci. **35**, 279.

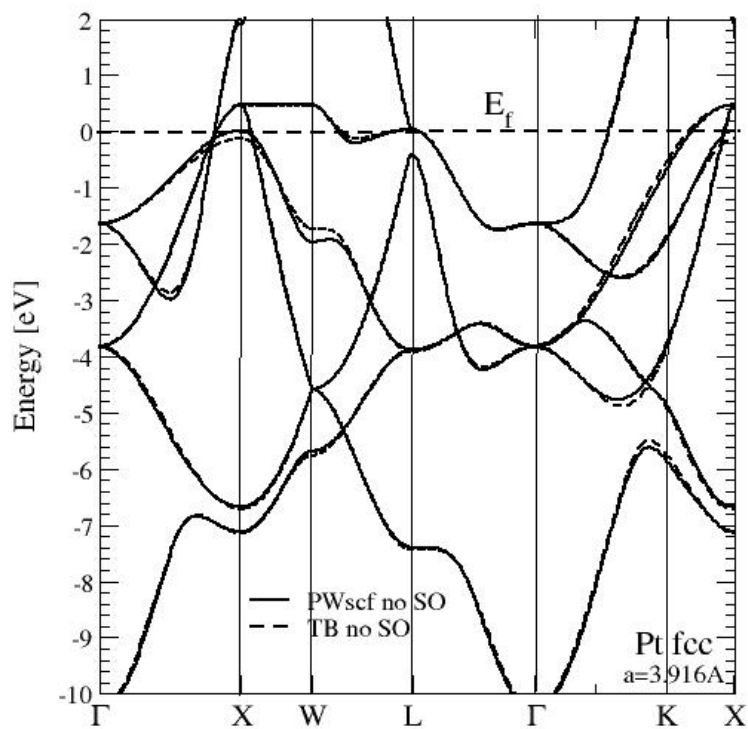


**Figure 1.** Band structure of fcc Pt without spin-orbit obtained from ab-initio and TB calculations for a lattice parameter of  $3.91\text{\AA}$

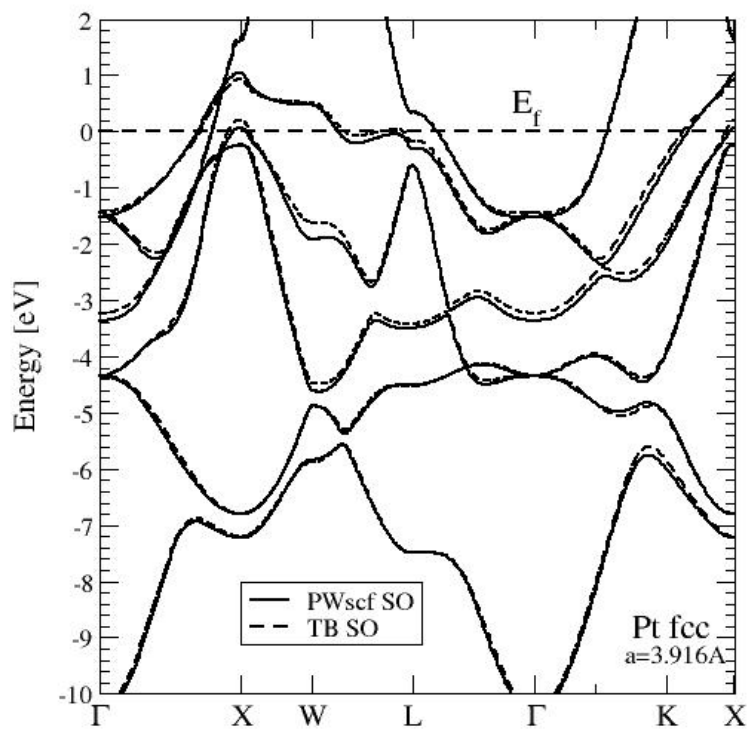


**Figure 2.** Same as Fig.1 but with spin-orbit.

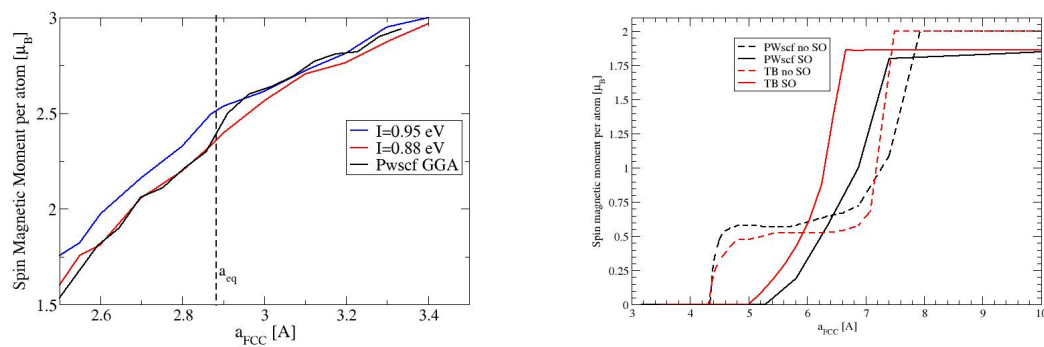


**Figure 3.** (color on line) Left part: spin magnetic moment of bcc Fe as a function of the lattice parameter from GGA and TB calculations for two values of  $I_d(\text{Fe})$ . Right part: spin magnetic moment of fcc Pt as a function of the lattice parameter from ab-initio and TB calculations with and without spin-orbit coupling.

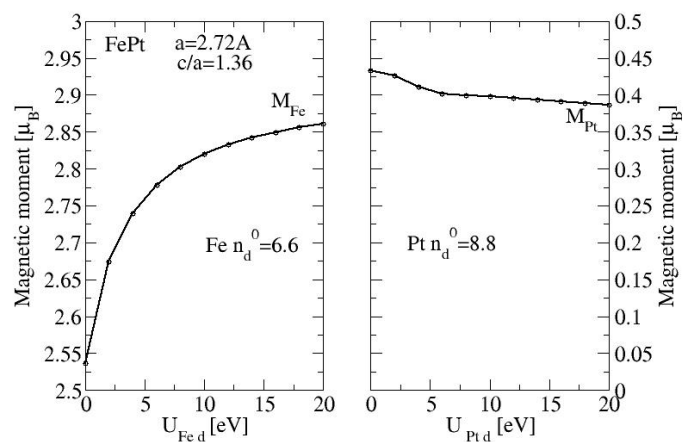


**Figure 4.** Spin magnetic moment in bulk  $L1_0$  FePt of Fe and Pt as a function of the value of  $U_{Fe,d}$  and  $U_{Pt,d}$  respectively

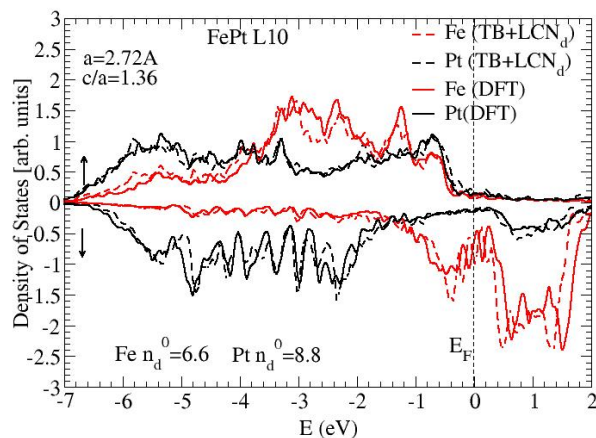


**Figure 5.** (color on line) Density of states projected by spin and site from TB and ab-initio calculations for bulk  $L1_0$  FePt.

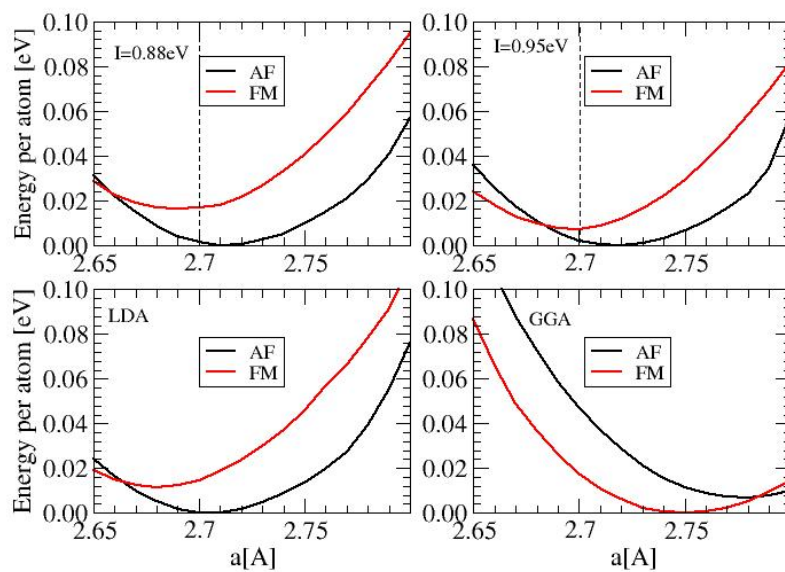


**Figure 6.** (color on line) upper part: energy per atom for AF and FM configurations of bulk  $L1_0$  FePt from TB calculations as a function of the lattice parameter for two values of  $I_d(Fe)$ . lower part: energy per atom for AF and FM configurations of bulk  $L1_0$  FePt as a function of the lattice parameter from LDA and GGA calculations.

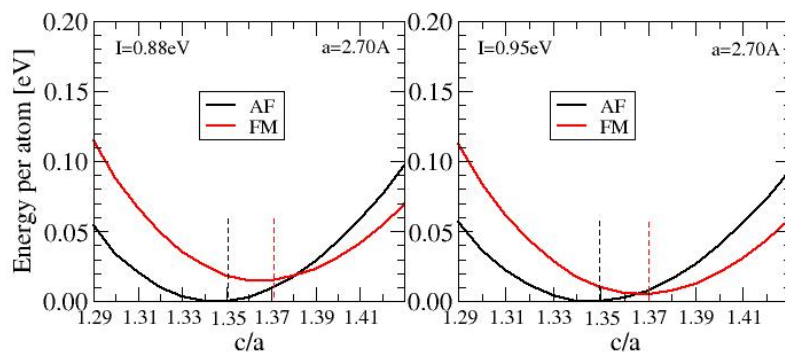


**Figure 7.** (color on line) Energy per atom of bulk  $\text{FePtL1}_0$  as a function of  $c/a$  for  $a=2.70\text{\AA}$  and two values of the Fe Stoner parameter

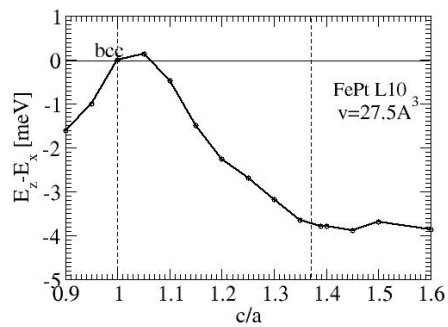


**Figure 8.** Calculated MAE of  $\text{L1}_0$  FePt as a function of the  $c/a$  ratio for a fixed volume.  $c/a = 1$  corresponds to the bcc structure for which the MAE almost cancels due to symmetry reasons.

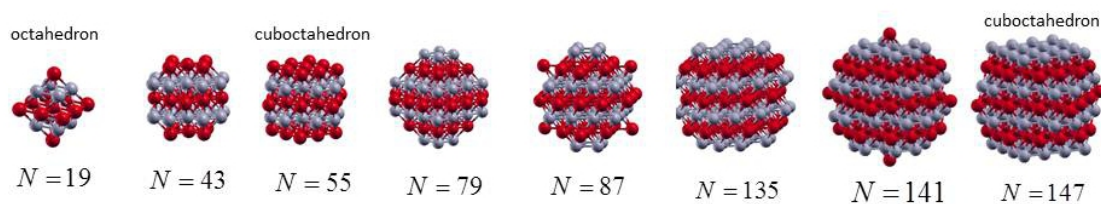


**Figure 9.** (color on line) Clusters of L1<sub>0</sub> FePt with an increasing number of atoms. Fe atoms appear in red and Pt in grey.

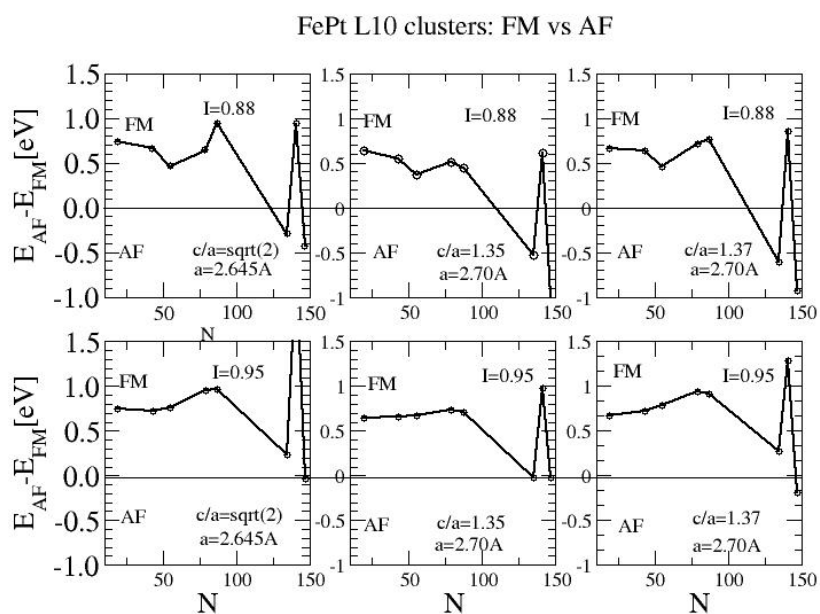


**Figure 10.** Energy difference between the AF and FM configurations of L1<sub>0</sub> FePt clusters as a function of their number of atoms and different values of  $c/a$  for for  $I_d(\text{Fe})=0.88$  (upper part) and  $I_d(\text{Fe})=0.95$  (lower part)



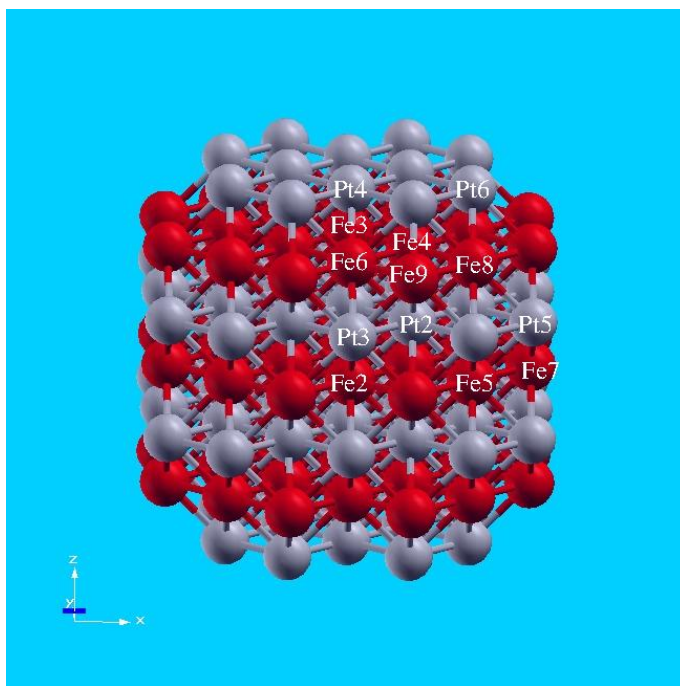


**Figure 11.** (color on line) labeling of some atoms in the  $L1_0$  FePt cluster with 135 atoms. The label increases with the distance from the considered atom to the cluster center. Fe atoms appear in red and Pt in gray.

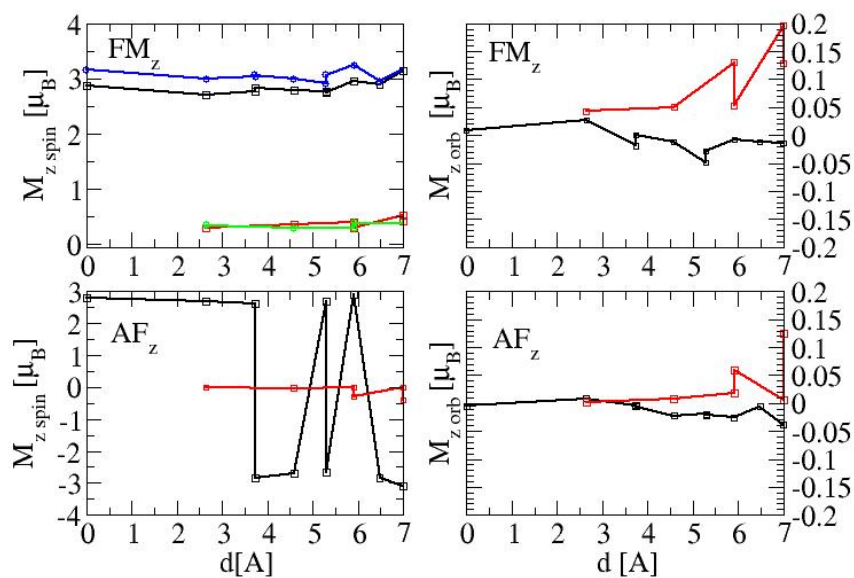


**Figure 12.** (color on line) Spin (left part) and orbital (right part) magnetic moments of Fe (in black) and Pt (in red) in the  $L1_0$  FePt cluster with 135 atoms as a function of the distance from the cluster center. Upper part FM configuration lower part AF configuration. The squares correspond to the atoms labeled in Fig.11. in the same order. In the upper left panel we have added the data points extracted from Fig. 1 of Ebert's paper[18], the DFT magnetic moments of Fe are in blue and the ones of Pt in green.

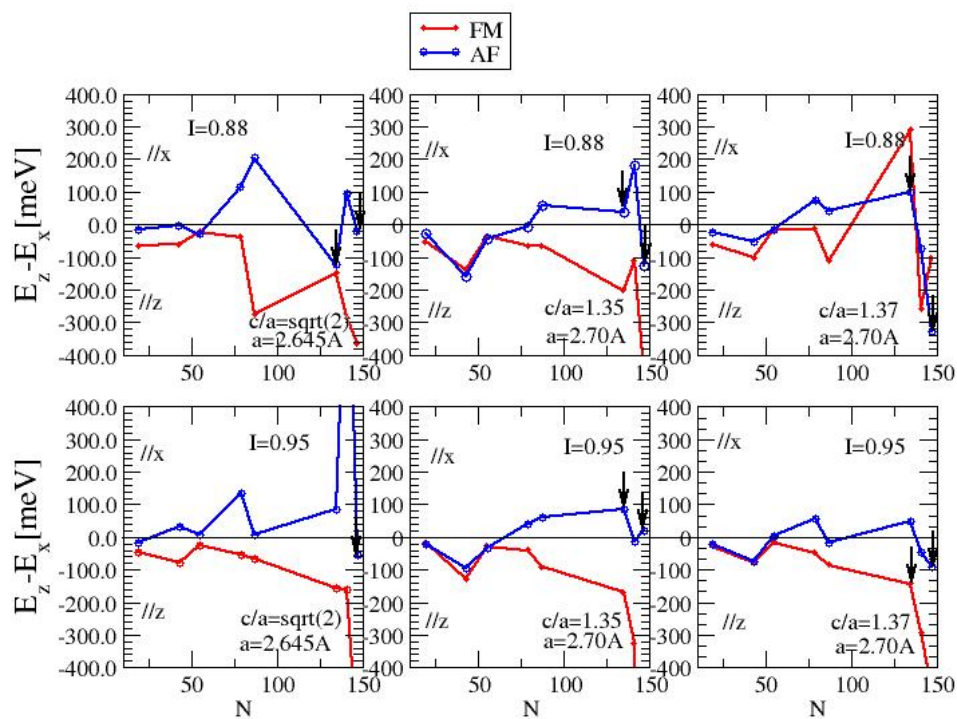


**Figure 13.** (color on line) MAE of  $\text{L1}_0$  FePt clusters as a function of their number of atoms and different values of  $c/a$  for  $I_d(\text{Fe})=0.88$  (upper part) and  $I_d(\text{Fe})=0.95$  (lower part).

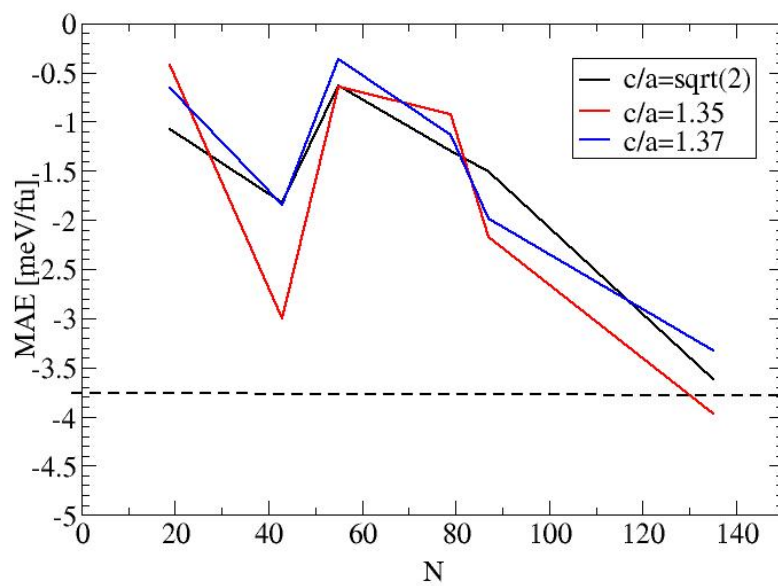


**Figure 14.** MAE of  $L1_0$  FePt clusters as a function of their number of atoms and different values of  $c/a$  for  $I_d(Fe)=0.95$ . The dashed line corresponds to the bulk  $L1_0$  FePt.